A Theoretical Investigation of the Ni(II)-Catalyzed Hydrovinylation of Styrene

Jorly Joseph,[†,‡] T. V. RajanBabu,*[,⊥] and Eluvathingal D. Jemmis*[,‡,§]

School of Chemistry, University of Hyderabad, Central University P. O., Hyderabad 500046, India, Department of Inorganic and Physical Chemistry, Indian Institute of Science, Bangalore 560012, India, Indian Institute of Science Education and Research, Thiruvananthapuram, CET Campus, Kerala 695016, India, and Department of Chemistry, The Ohio State University, 100 W. 18th Avenue, Columbus, Ohio 43210

Received January 20, 2009

We report a detailed and full computational investigation on the hydrovinylation reaction of styrene with the Ni(II)-phospholane catalytic system, which was originally presumed to proceed through a cationic mechanism involving a nickel hydride intermediate. The following general features emerge from this study on a specific catalyst complex that was found to give quantitative yield and moderate selectivity: (a) the activation barrier for the initiation (18.8 kcal/mol) is higher than that for the reaction due to a low-lying square-planar pentenyl chelate intermediate originating from a Ni(II)-allyl catalyst precursor. Consequently there is an induction period for the catalysis; (b) the exit of product from the catalyst is via a *β-H-transfer* step instead of the usual *β-H elimination* pathway, which has a very high activation energy due to a trans effect of the phospholane ligand; (c) the turnover-limiting and enantio- determining transition state is also the β-H-transfer; (d) because of the absence of a hydride intermediate, the unwanted isomerization of the product is prevented; (e) since the enantio-discrimination is decided at the H-transfer stage itself, the configuration of the product in a catalytic cycle influences the enantioselectivity in the subsequent cycle; (f) the trans effect of the sole strong ligand in the d^8 square-planar Ni(II), the stability of the η^3-benzyl intermediate, and the availability of three coordination sites enable regioselective hydrovinylation over the possible oligomerization/polymerization of the olefin substrates and linear hydrovinylation. This work has also confirmed the previously recognized role of the hemilabile group at various stages in the mechanism.

Introduction

Among the Ni(II)-catalyzed olefin dimerization reactions, the hydrovinylation reaction, viz., the addition of a vinyl group and a hydrogen across a double bond (Scheme 1), has attracted the most attention.[1] Since the branched product is chiral, a regio- and stereoselective version of this reaction could provide easy access to a variety of olefin-derived products including carboxylic acid derivatives. For example, the hydrovinylation of vinylarene derivatives that leads to 3-arylbutenes could be used for the synthesis of widely used anti-inflammatory 2-arylpropionic acids such as ibuprofen and naproxen. Even though the hydrovinylation reaction has had a long history dating back to 1965, until recently no catalyst system gave satisfactory yield and selectivity to be of practical value. The use of high pressures of ethylene and metal components incompatible with sensitive organic groups were also major limitations of many of the initially reported procedures. In addition, isomerization of the primary products and oligomerization of the vinylarene and ethylene were other detractions of this powerful reaction (Scheme 1).

Since our initial disclosure of new protocols for this reaction (Scheme 2),[2] its scope has been considerably broadened. Application of old (Figure 1: **L1**, **L2**,**L3**) and new (**L4**, **L5**, **L6**) ligands has enabled successful asymmetric hydrovinylation of vinyl arenes,[3] 1,3-dienes,[3i,4] and strained bicyclic olefins such as norbornene.[3f,5] Several examples are illustrated in eqs 1−3.

* Corresponding authors. E-mail: jemmis@iisertvm.ac.in, rajanbabu.1@osu.edu.

[†] University of Hyderabad.

[‡] Indian Institute of Science.

[§] Indian Institute of Science Education and Research.

[⊥] The Ohio State University.

(1) For a history of the reaction, a proposed mechanism, the scope, and its limitations, see: (a) RajanBabu, T. V. *Chem. Rev.* **2003**, *103*, 2845. See also: (b) Jolly, P. W.; Wilke, G. In *Applied Homogeneous Catalysis with Organometallic Compounds*; Cornils, B., Herrmann, W. A., Eds.; VCH: New York, 1996; Vol. 2, p 1024. (c) RajanBabu, T. V. *Synlett* **2009**, 853.

(2) (a) Nomura, N.; Jin, J.; Park, H.; RajanBabu, T. V. *J. Am. Chem. Soc.* **1998**, *120*, 459. (b) RajanBabu, T. V.; Nomura, N.; Jin, J.; Radetich, B.; Park, H.; Nandi, M. *Chem.−Eur. J.* **1999**, *5*, 1963. (c) RajanBabu, T. V.; Nomura, N.; Jin, J.; Nandi, M.; Park, H.; Sun, X. *J. Org. Chem.* **2003**, *68*, 8431.

(3) Use of Wilke's *Azaphospholene* (**L1**): (a) Wegner, A.; Leitner, W. *Chem. Commun.* **1999**, 1583, and references therein. Phospholanes as ligands: (b) Nandi, M.; Jin, J.; RajanBabu, T. V. *J. Am. Chem. Soc.* **1999**, *121*, 9899. (c) Zhang, A.; RajanBabu, T. V. *Org. Lett.* **2004**, *6* 1515. Phosphiniates: (d) Park, H.; RajanBabu, T. V. *J. Am. Chem. Soc.* **2002**, *124*, 734. Phosphoramidites: (e) Franció, G.; Faraone, F.; Leitner, W. *J. Am. Chem. Soc.* **2002**, *124*, 736. (f) Park, H.; Kumareswaran, R.; RajanBabu, T. V. *Tetrahedron* **2005**, *61*, 6352. (g) Shi, W.-J.; Zhang, Q.; Xie, J.-H.; Zhu, S.-F.; Hou, G.-H.; Zhou, Q.-L. *J. Am. Chem. Soc.* **2006**, *128*, 2780. (h) Zhang, A.; RajanBabu, T. V. *J. Am. Chem. Soc.* **2006**, *128*, 5620. (i) Smith, C. R.; RajanBabu, T. V. *Org. Lett.* **2008**, *10*, 1657. (j) Details of preparative methods: Smith, C. R.; Zhang, A.; Mans, D. J.; RajanBabu, T. V. *Org. Synth.* **2008**, *85*, 248.

(4) (a) Zhang, A.; RajanBabu, T. V. *J. Am. Chem. Soc.* **2006**, *128*, 54. (b) Saha, B.; Smith, C. R.; RajanBabu, T. V. *J. Am. Chem. Soc.* **2008**, *130*, 9000.

(5) Kumareswaran, R.; Nandi, N.; RajanBabu, T. V. *Org. Lett.* **2003**, *5*, 4345.

10.1021/om900045p CCC: $40.75
Publication on Web 05/20/2009

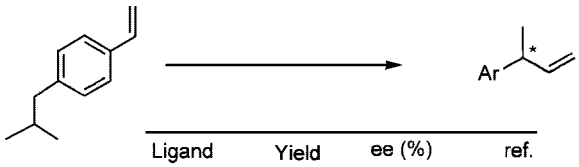

Ligand	Yield	ee (%)	ref.
L1	44	89 (*R*)	3a
L5	99	91 (*R*)	3c
L6	97	96 (*S*)	3i

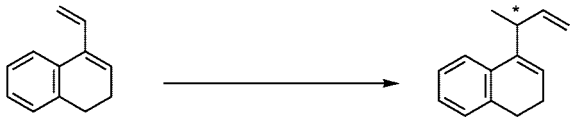

Ligand	Yield	ee (%)	ref.
L5	99	93 (*R*)	4a
L3	99	99 (*S*)	4a

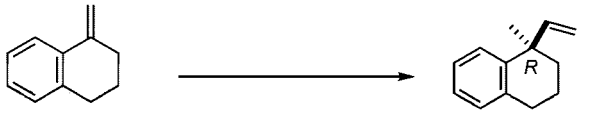

Ligand	Yield	ee (%)	ref.
L3	70	99 (*R*)	3h
L6	79	99 (*R*)	3i

Mechanism of Ni-Catalyzed Hydrovinylation of Vinylarenes. Even though much of the early studies of hydrovinylation of styrene are characterized by a lack of any selectivity, many of them provide significant mechanistic insights into the reaction. For example, kinetic and solvent effect studies of hydrovinylation with $NiX_2/AlEt_3/BF_3 \cdot OEt_2/P(OPh)_3$[6a−c] provided some early indications of the $[Ni-H]^+$ coordination to a styrene and subsequent addition. The deactivating effect of a solvent was found to increase in the order CH_2Cl_2, PhF, PhCl, PhMe, $PhNO_2$, Et_2O, consistent with the inhibitory effect of a coordinating Lewis base. Electron-withdrawing substituents on styrene retard the reaction rate. Studies of D-distribution in the product when the hydrovinylation was carried out with $D_2C{=}CD_2$ provided further evidence for the involvement of a cationic nickel hydride intermediate.[6c] Even though a catalytically active $L_n[Ni-H]^+$ has not been isolated, its generation and inter-[7] and intramolecular[8] additions have been documented. Since these early studies, Brookhart and DiRenzo[9] have provided more details of their mechanistic study of closely related Pd-catalyzed codimerization of styrene and ethylene.

Mechanistically one of the most significant early observations that we made[3b] was the total inability of chelating phosphines to effect the reaction under our standard protocol. One such example is shown in Scheme 2. The chelating bisphosphine **1′** gave no trace of coupling products, whereas ligand **1**, carrying one chelating phosphorus and a hemilabile −OMe group, gave a quantitative yield of the product in ∼42% ee at −45 °C using 0.014 equiv of the precatalyst under 1 atm of ethylene. All ligands that have yielded useful levels of asymmetric induction in the hydrovinylation reaction share this common structural feature.[3] In this connection, we also recognized[3b] a strong synergy between a hemilabile ligand and a highly dissociating counterion {e.g., $[3,5\text{-}(CF_3)_2C_6H_3]_4B$, Scheme 2}. In the absence

Scheme 1. Hydrovinylation of Vinylarenes

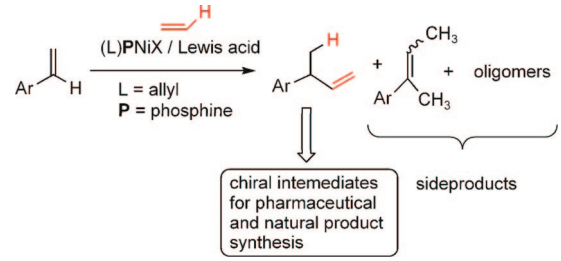

Scheme 2. Asymmetric Hydrovinylation Using Hemilabile Ligands

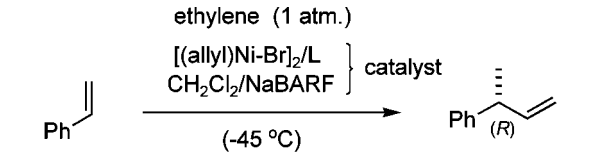

L	yield (%)	(%ee)
1	>98	42 (*R*)
1'	0	--

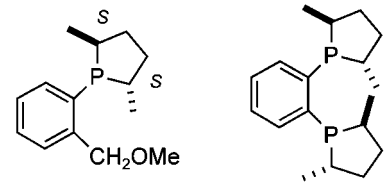

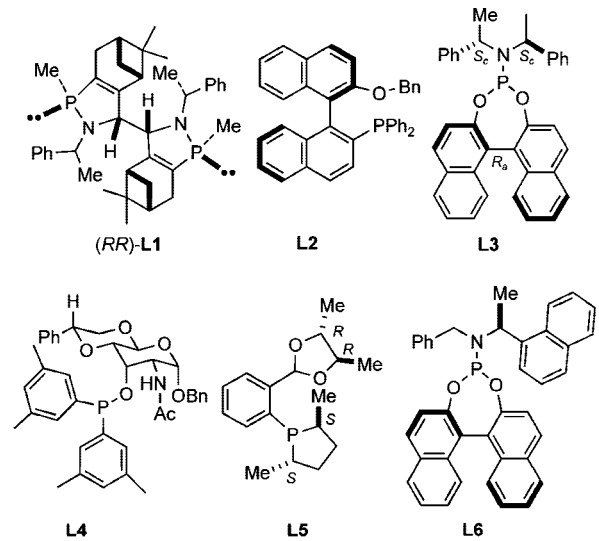

Figure 1. Assorted ligands used for asymmetric hydrovinylation.

(6) (a) Azizov, A. G.; Mamedaliev, G. A.; Aliev, S. M.; Aliev, V. S. *Azerb. Khim. Zh.* **1978**, *3*, 6002; *Chem. Abstr.* **1979**, *90*, 6002. (b) Azizov, A. G.; Mamedaliev, G. A.; Aliev, S. M.; Aliev, V. S. *Azerb. Khim. Zh.* **1979**, *3*. *Chem. Abstr.* **1980**, *93*, 203573. (c) Mamedaliev, G. A.; Azizov, A. G. *Polym. J. (Tokyo, Jpn.)* **1985**, *17*, 1075.

(7) Wilke, G. *Angew. Chem., Int. Ed. Engl.* **1988**, *27*, 185.

(8) Muller, U.; Keim, W.; Krüger, C.; Betz, P. *Angew. Chem., Int. Ed.* **1989**, *28*, 1011.

(9) DiRenzo, G. M. Mechanistic Studies of Catalytic Olefin Dimerization Reactions Using Electrophilic η^3-allyl-Palladium(II) Complexes, Ph.D. Thesis, University of North Carolina, 1997. We thank Professor Brookhart and Dr. DiRenzo for a copy of this dissertation.

Scheme 3. Proposed Mechanism of Hydrovinylation of Styrene

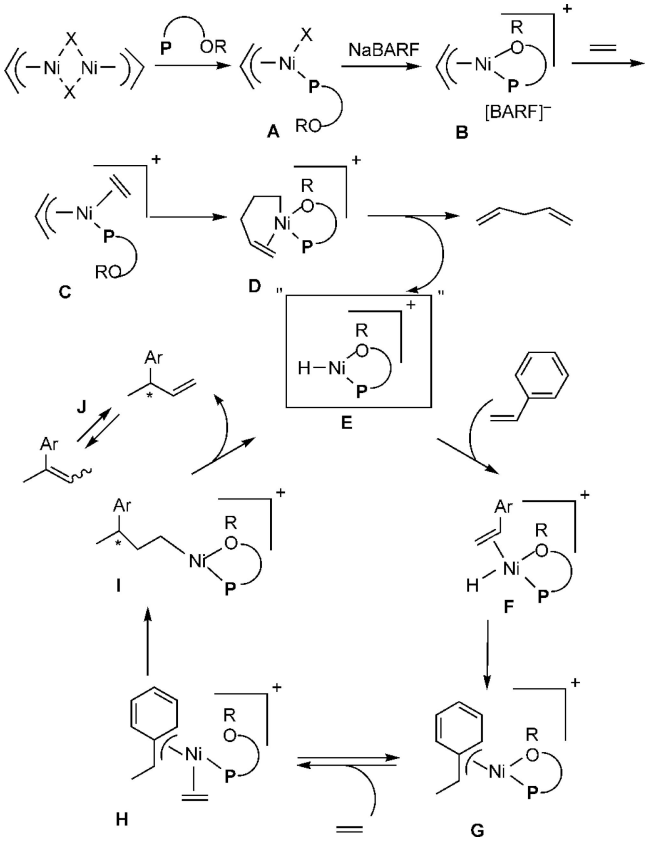

of a hemilabile ligand, a coordinating counterion such as triflate ($CF_3SO_3^-$) is essential for the success of the reaction.

In this computational probe, we explore the reaction depicted in Scheme 2, which uses the ligand **1**. The reaction under these conditions was chosen for detailed study because it represents a minimalist catalyst system that gives significant enantioselectivity, yet small enough to be amenable to extensive ab initio study. A study of this reaction, we hope, would allow the delineation of the basic mechanism and at the same time revealing the possible origin of the stereoselectivity.

At the outset of the synthetic studies we relied on a "working model" for the mechanism of the reaction as shown in Scheme 3. In this model, the functional equivalent of a catalyst is represented by **E**, shown within quotations inside a square box. This representation is meant to emphasize the point that this cationic metal hydride intermediate, associated with a noncoordinating counteranion and a phosphine, is highly speculative. The active catalyst precursor **B** is produced from a reaction of allylnickel bromide dimer and ligand **1** with one hemilabile donor atom, followed by abstraction of the bromide by NaBARF. Several crystal structures of complexes related to Ni-allyl compounds **A** and **B** are known with phosphines, Cy_3P [X = $MeAlCl_3$],[10a] P(menthyl)(Me)(Bu^t) [X = Cl],[10b] P(menthyl)$_2$(Me) [X = Me].[10c] and [*o*-MeOC(O)-C_6H_4]-PPh_2.[10d] The crucial metal hydride **E** is formed by (a) ligand substitution of the hemilabile group of **B** by ethylene to form **C** and (b) insertion of ethylene into the allyl−Ni bond followed by (c) a β-hydride elimination. Addition of the metal hydride to the vinylarene would lead to the benzyl complex **G**, which is shown as a 16-electron η^3-structure. Ligand substitution with ethylene leads to **H**. At higher concentrations of ethylene and styrene this species could serve as a catalyst resting state. Strong evidence for such a situation has been provided by Brookhart and Direnzo[9] in mechanistically related [(allyl)Pd(Cy_3P)]$^+$-[BARF]$^-$ mediated dimerization of styrene. Insertion of ethylene followed by β-hydride elimination from **I** regenerates the metal hydride catalyst **E** and the product, 3-aryl-1-butene. Enantioselectivity in the reaction could arise from diastereoselective addition of metal hydride to styrene (**E** → **G**) when the ligand is chiral and nonracemic. A number of anecdotal observations reported in the literature and some made during our studies can be accommodated by this mechanism.

(a) Diminished reactivity of electron-deficient vinylarenes might arise from low rate of metal hydride addition (**E** →**G**).

(b) Deactivating effects of the coordinating solvents.

(c) The observed isomerization of the initially formed 3-aryl-1-butene to 2-aryl-2-butene with some catalytic systems could be mediated by the metal hydride via sequential addition−elimination reactions.

(d) Total inhibition of the reaction by chelating phosphines.

In this work, we will examine each step in the mechanism (or alternatives if the step was found to be energetically unfavorable) to reveal the exact nature of the transition states and intermediates, and estimate the activation barriers for critical steps. We will also attempt to determine the origin of asymmetric induction in the reaction.

Details of the Computational Methods

The problem at hand is computationally very demanding, and unless otherwise mentioned, we are forced to restrict the calculations to the B3LYP/6-31G* level, available in the Gaussian package.[11] This is quite a reasonable level[12] and has been used previously by Leitner et al. to examine the last stages of asymmetric hydrovinylation catalyzed by Ni(II)-phosphoramidite complexes.[13] All reported energies are in kcal/mol and include zero-point energy (ZPE) at the optimized level. We employed the following strategy for the exploration of the reaction paths to track the vast potential energy surface: a detailed conformational search has been made only for the crucial transition states and their previous lowest energy intermediates so as to get exact activation energies for all the important steps. For all other "connecting" transition states (and intermediates) involved in the reaction path, either at least one conformer was located whose energy lies in between the above identified lowest intermediate and transition state, or some obvious low-lying (mainly rotational) transition states/intermediates were ignored. We shall illustrate this using Figure 2, which summarizes the results (vide infra). All points in Figure 2 representing key

(10) (a) Bogdanović, B.; Henc, B.; Lösler, A.; Meister, B.; Pauling, H.; Wilke, G. *Angew. Chem., Int. Ed. Engl.* **1973**, *12*, 954. (b) Brandes, H.; Goddard, R.; Jolly, P. W.; Krüger, C.; Mynott, R.; Wilke, G. *Z. Naturforsch.* **1984**, *39B*, 1139. (c) Barnett, B. L.; Krüger, C. *J. Organomet. Chem.* **1974**, *77*, 407. (d) Bonnet, M. C.; Dahan, F.; Ecke, A.; Keim, W.; Schulz, R. P.; Tkatchenko, I. *J. Chem. Soc., Chem. Commun.* **1994**, 615.

(11) Frisch, M. J.; et al. *Gaussian 03*; Gaussian, Inc.: Pittsburgh, PA, 2003 (See Supporting Information for a complete list of authors).

(12) We have also checked the effect of diffuse functions, as per the suggestion of one of the referees, on the energetics of two important steps at B3LYP/6-31+G*//B3LYP/6-31G* (and also at B3LYP/6-31+G*; given in parentheses below). The energy difference for **40** viz., **40S** – **40R** [vide infra, see text] changes from –0.6 kcal/mol to –0.5 (–0.6) kcal/mol in the same direction. So is the case for **99**, viz., **99RS** – **99RR**, which is now –0.4 (0.3) kcal/mol versus the previous –0.6 kcal/mol. The new activation energy for initiation is 19.2 (18.6) kcal/mol for **S** versus the earlier 18.8 kcal/mol, and for **R** 19.8 (19.2) kcal/mol versus the earlier 19.5 kcal/mol. The activation energy, **99RS** – **86R**, of the catalytic cycle is now 15.2 (14.8) kcal/mol versus the previous 17.0 kcal/mol. The corresponding **99RR** – **86R** is 15.6 (15.0) kcal/mol versus the previous 17.6 kcal/mol.

(13) (a) Hölscher, M.; Franciò, G.; Leitner, W. *Organometallics* **2004**, *23*, 5606. For a limited molecular model study, see: (b) Angermund, K.; Eckerle, A.; Lutz, F. Z. *Naturforsch., B: Chem. Sci.* **1995**, *50*, 488.

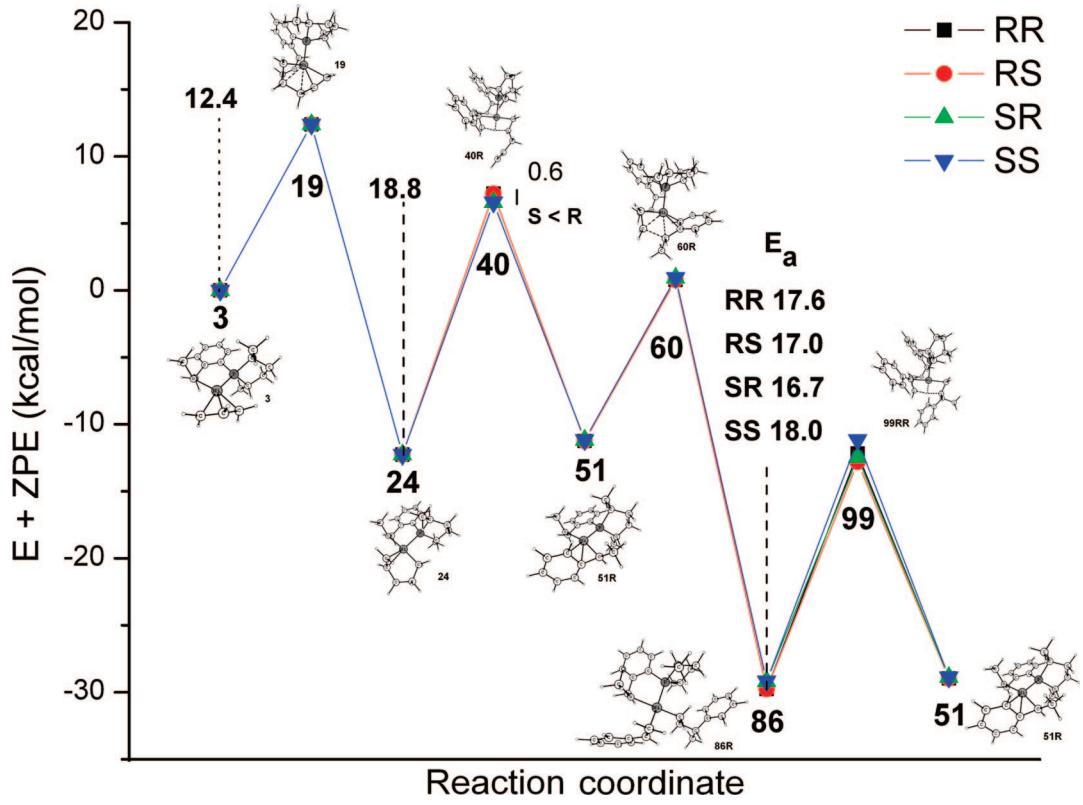

Figure 2. Summary of the reaction. The structures shown are for one series; other structures can be found in the article.

intermediates and transition states and the structures shown represent the lowest conformers of these species in the reaction.[14] The reaction path connecting two points, one minimum (intermediate) and one maximum (transition state), was confirmed to lie in between them.

To find out which two intermediates are connected by a transition state, we applied a frequency following method. This was done by first obtaining the geometries by a very small displacement of the imaginary vibrational mode of the transition state in either directions, and then both were optimized by calculating the force constants at all optimization steps.

To avoid cluttering in the schemes depicting reaction paths, two types of arrows are used to connect an intermediate to a transition state (and vice versa). A "single" arrow means the two neighboring species are directly connected, while a "double" arrow means either another conformer of the intermediate connects to the transition state or some steps that are already described are involved, or some of the trivial steps are skipped in the drawing. The equilibrium arrows in the schemes have the usual connotation, so do square brackets that envelop the transition state structures. The additional # symbol signifies the highest transition state in the reaction steps under consideration. The images of all structures shown in the article were generated using ChemCraft software.

Results and Discussion

Generation of the Active Catalyst. Scheme 4 shows the generation of active catalyst precursors from $[(allyl)Ni\text{-}Br]_2$ and ligand **1**. The experiments reveal[3b] that there is only one diastereomer (either **3** or **3′**) present before the start of the hydrovinylation reaction, and we attempted to identify which of these could be present, because it is the first chiral organometallic intermediate in the catalytic process and thus has the potential to affect the eventual stereochemical outcome of the reaction. The difference in energy between **3** and **3′** is only 0.4 kcal/mol (in favor of **3**), which is low enough for both to be observed if there is an equilibration between them after they have been generated. To refine the relative energies, we did the calculation at the B3LYP/6-311++G** level, where the result was further validated (0.5 kcal/mol). The activation energy for their interconversion is 23.8 kcal/mol, which is large and rules out a rapid equilibrium causing the single peak observed in the ^{31}P NMR at room temperature and below. That means formation of one of these diastereomers (either **3** or **3′**) is favored over the other. Below this, diastereomer **3** is located; we use the available experimental NMR results for the corroboration of our arguments.

Scheme 4. Generation of Precatalysts (2, 2′; 3, 3′)

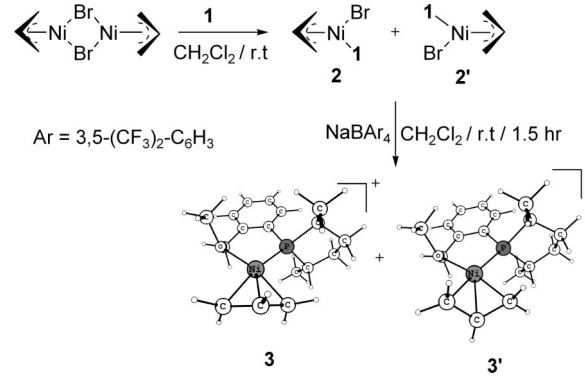

Effect of an Extra Ligand on the Equilibration of the Square-Planar Diastereomers 2 and 2′. The starting nickel salt, $[(allyl)Ni\text{-}Br]_2$, is expected to yield two diastereomers, **2**

(14) This conformational search was carried out using the known bonding pattern of the system, which has only the usual chemical bonds; thus the search involved rotation across the bonds. A number of conformers of very close energy to the lowest conformer exist for many of the points in Figure 2. These were ignored from consideration for the discussion, although they are also populated.

Scheme 5. Energetics of Interconversion between the Diastereomers of 2 and 5: Effect of Hemilabile Coordination

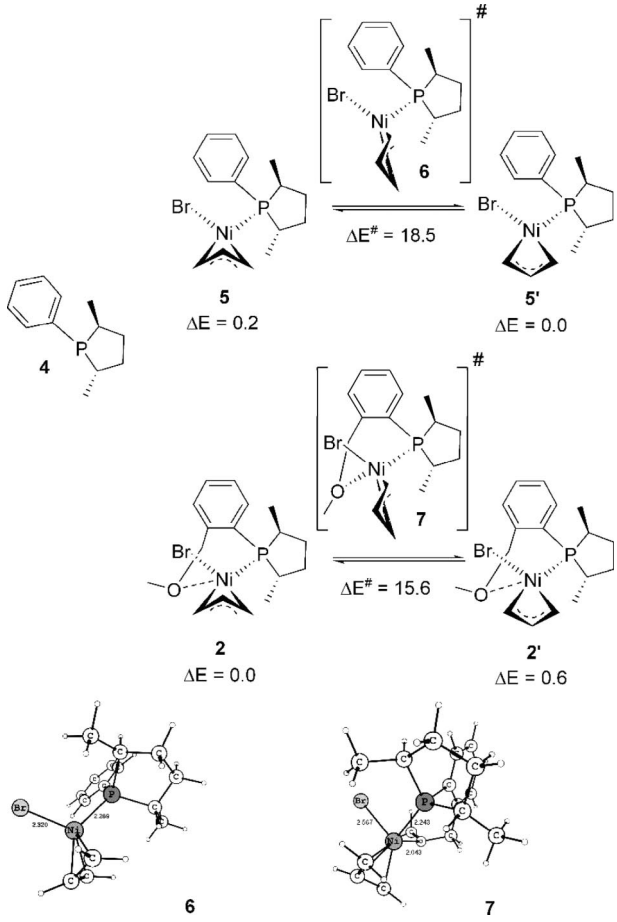

and **2′** (Scheme 4), upon reaction with ligand **1**. The ^{31}P NMR shows a single peak at room temperature, but reveals the presence of another diastereomer at lower temperatures, 3:1 at −20 °C and 4:1 at −80 °C.[3b] Insight into this isomerization reaction can be gleaned by looking at a closely related system containing the ligand **4**, *without the extra ligating* −OMe group, and the corresponding square-planar complexes **5** and **5′** (Scheme 5). These complexes are found in a ratio of approximately 1:1 at temperatures between 27 and −70 °C. We find that the extra (hemilabile) ligating group in **1** affects not only the rate of interconversion between **2** and **2′** but also the equilibrium constant (Scheme 5). Ligand **4**, without any such group, makes both diastereomers virtually iso-energetic (ΔE = 0.2 kcal/mol, corresponds to 1.4:1.0 at 300 K), so even if there is an equilibrium between **5** and **5′**, they appear in an approximate ratio of 1:1.[3b] The activation energy, 18.5 kcal/mol, is low enough, but a slow interconversion at room temperature occurs. At lower temperatures, the interconversion is more difficult, and hence the same ratio at room temperature prevails. In contrast, ligand **1** does distinguish the diastereomers energetically (ΔE = 0.6 kcal/mol, corresponding to 2.7:1.0 at 300 K) because of the fifth coordination via oxygen and to the exo/endo effect of the η^3-allyl for a d^8 square-planar complex.[15] Endo (**2′**) (O endo to the central C−H bond of η^3-allyl) is higher in energy compared to exo (**2**) because both O and the central C compete for the same orbitals of Ni. The extra ligand also makes interconversion between **2** and **2′** faster by allowing the otherwise tetrahedral transition state **6** to change to a pseudo-square-planar (to be exact, square pyramidal allowing for the weak O/Br coordinations) transition state **7**, a preferred geometry for a d^8 electronic configuration. The square plane of **7** involves

Scheme 6. Formation of Sole Active Catalyst Precursor 3 from 2 and 2′

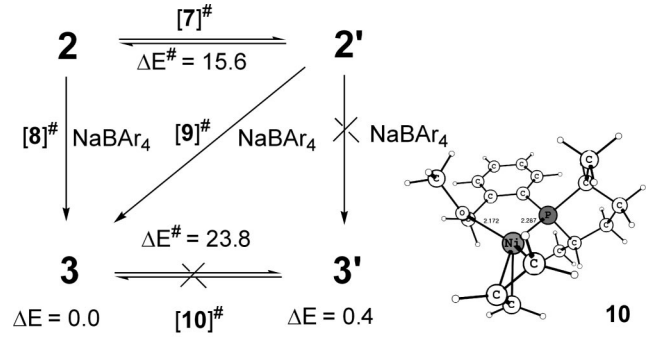

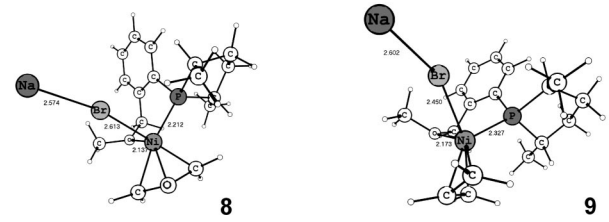

P, O, and η^3-allyl, as shown in Scheme 5, and Br occupies the axial position if we consider it as a square pyramid. Thus the extra ligand lowers the barrier to 15.0 kcal/mol. So the single peak at room temperature[3b] must correspond to coalescence. The lower barrier allows it to readjust the equilibrium ratio at lower temperatures, unlike with ligand **4**.

Formation of 3 and 3′ by Bromide Abstraction. Why Only One Diastereomer? Despite the presence of both diastereomers (**2** and **2′**), and the possibility of interconversion between them, we found that the feasible path for Br abstraction precludes **3′** from being formed, so the sole diastereomer present initially is **3**. This is because the expulsion of Br assisted by Na^+ has the lowest energy in an endo route. Thus both initial diastereomers **2** and **2′** can give only **3** via the respective endo transition states **8** and **9** (Scheme 6). The orientation of the allyl unit with respect to the exiting Br is the principal difference between these two transition states. The dihedral angle Br−Ni−C$^2_{allyl}$−H is −33° in **8** (transition state from **2**) and 54° in **9** (transition state from **2′**). Upon coordination of Na with Br, the Ni−Br bond is weakened. Now the NaBr is able to exit via a turnstile rotation[16a] of η^3-allyl, as shown in Scheme 6. Achieving transition state **8** is easier than transition state **9** since the latter has to undergo considerably more rotation with respect to **2′** to reach the endo arrangement. The energy difference between **8** and **9** is 5.9 kcal/mol. Since a reasonable estimation of the activation energy is difficult because of the charge separation between the intermediate and transition state, it is not certain whether **9**, which is higher than **8**, is actually

(15) (a) For a recent DFT study: Ariafard, A.; Lin, Z. *Organometallics* **2005**, *24*, 3800. For previous theoretical studies of bonding in allyl systems, see: (b) Albright, T. A.; Hofmann, P.; Hoffmann, R. *J. Am. Chem. Soc.* **1977**, *99*, 7546. (c) Harlow, R. L.; McKinney, R. J.; Ittel, S. D. *J. Am. Chem. Soc.* **1979**, *101*, 7496. (d) Mingos, D. M. P. In *Comprehensive Organometallic Chemistry*; Wilkinson, G., Ed.; Pergamon: Oxford, England, 1982; Vol. 3, Chapter 19, pp 60−67. (e) Goddard, R.; Krüger, C.; Mark, F.; Stansfield, R.; Zhang, X. *Organometallics* **1985**, *3*, 285.

(16) (a) Rufinska, A.; Goddard, R.; Weidenthaler, C.; Buhl, M.; Porschke, K.-R. *Organometallics* **2006**, *25*, 2308. Allyl rotation mechanism in Ni(II) complexes: (b) Hampton, P. D.; Wu, S.; Alam, T. M.; Claverie, J. P. *Organometallics* **1994**, *13*, 2066. (c) Aresta, M.; Quaranta, E.; Dibenedetto, A.; Giannoccaro, P.; Tommasi, I.; Lanfranchi, M.; Tiripicchio, A. *Organometallics* **1997**, *16*, 834. (d) Aresta, M.; Dibenedetto, A.; Quaranta, E.; Lanfranchi, M.; Tiripicchio, A. *Organometallics* **2000**, *19*, 4199.

Scheme 7. Interconversion between 3 and 3′ via a Turnstile Rotation with the Help of Ethene

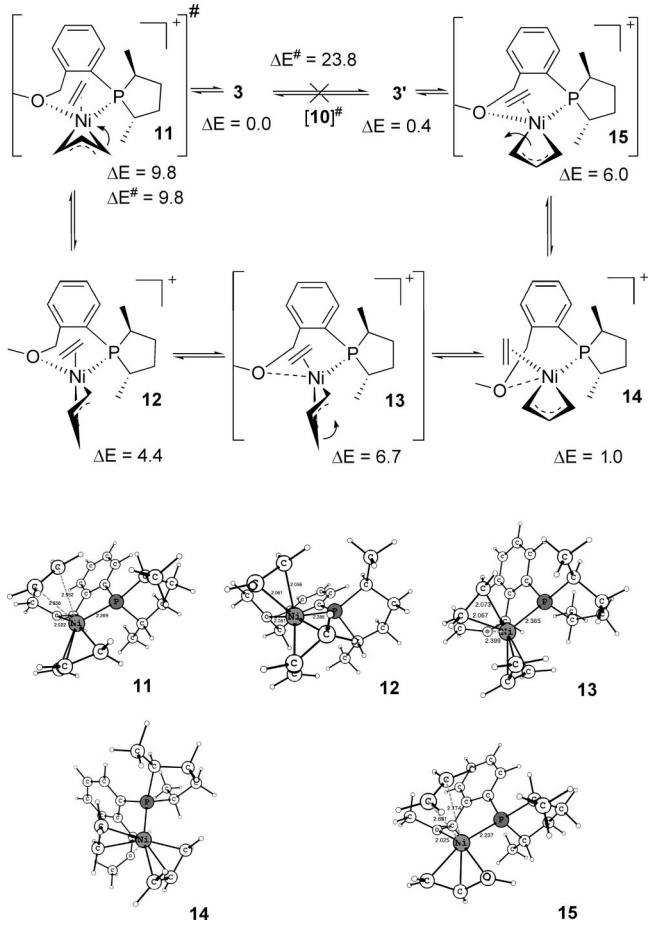

involved. We conclude that if the barrier for **9** is less than 15.0 kcal/mol, the activation energy for the conversion of **2′** to **2**, transition state **9** is involved in the formation of **3**; otherwise **3** is obtained through transition state **8** even from **2′** (via **2**). As pointed out before, the diastereomer **3′** is only 0.4 kcal/mol higher than **3**, but its generation from **3** is also prohibited because it involves a barrier (**10**) of 23.8 kcal/mol. (It may be noted that transition state **10** is remarkably higher than analogous, but neutral tetrahedral transition state **6**.) Thus we conclude that **3** is the active catalyst precursor present before the addition of substrates, ethene and styrene.

Interconversion of Diastereomers 3 and 3′ in the Presence of Ethene, an Extra Ligand. Since in the presence of an extra ligand allyl interconversion is easier in neutral **2** and **2′** (Scheme 5), we examined whether an added olefin makes interconversion of cationic **3** and **3′** feasible and hence nullify any possible consequences of the absence of the diastereomer **3′** initially. As anticipated, we found that ethene lowers the barrier for interconversion between **3** and **3′** via a turnstile rotation route, **15** (Scheme 7). The barrier for interconversion is only 9.8 kcal/mol (at 0 K). Even if we consider the additional entropy disadvantage of ethene association, it is still low enough for their interconversion at −45 °C, where the reaction was conducted. The catalyst precursor **3** can incorporate the ethene via transition state **11**, which involves the allyl ligand rotating counterclockwise to reach the intermediate **12**, which may be considered a square pyramid with P at the axial position. Continued allylic rotation at intermediate **12** leads to **14** via transition state **13**. Note that now oxygen is endo to η^3-allylic central C−H (dihedral angle O−Ni−C^2_{allyl}−H = 14° in **14**) and

Scheme 8. Generation of the Active Catalyst: (I) An Unlikely High-Energy Dissociative Initiation Path

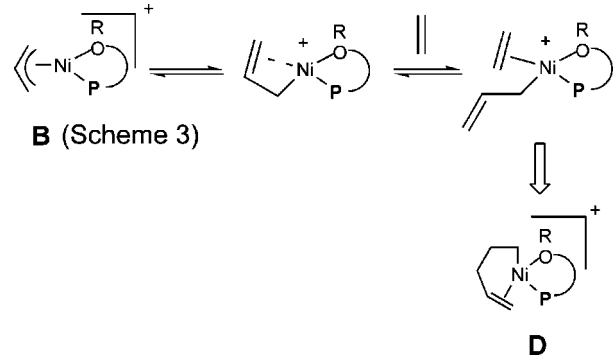

hence that the bond is weakened. The intermediate **14** is nothing but ethene incorporated in **3′** by the replacement of hemilabile O; that is, ethene ejection from **14** will give **3′**.

Although the coordinating ability of O is weak (**S1**, Scheme S1, Supporting Information), compared to styrene (**S3**, Scheme S1), for the cationic square-planar Ni(II) complex, in this particular ligand system that inherent advantage of styrene has been lost possibly to steric effects, so only **3** and to a lesser extent **3′** are present at the beginning of the hydrovinylation reaction. The lowest among the olefin complexes, the ethene complex (**S6**, Scheme S2), is only 0.4 kcal/mol lower than **3** despite having an additional (weak) ligation by O in the cationic complex. Considering the entropy effect it can be concluded that none of the olefin complexes have high concentrations in comparison with **3** (or **3′**).

Mechanism of Hydrovinylation

Initiation. Since at least two coordination sites on a Ni(II) complex are required for the reaction, and our precursor **3** has only one vacant site in the form of a hemilabile ligation, the first requirement is to enable at least one more site. As outlined in the mechanism, a C−C coupling with the η^3-allyl will do just that. One conceptual problem with the C−C bond formation via insertion of ethylene into the allyl−Ni bond (see mechanism, Scheme 3: **C** → **D**) is that it leads to a three-coordinated cationic intermediate and consequent large activation barrier, a disadvantage for the reaction at low (−45 to −77 °C) temperatures. So it is important to investigate how the catalytic system takes care of this problem. An alternate path that begins with η^1−η^3 slippage of the allyl unit followed by ligand substitution of the alkene (Scheme 8) could not be located because of the strong preference of the allyl unit to remain in the η^3 mode when two coordination sites are available in a d^8 square-planar complex.

Role of the Hemilabile Group. The labile ligand has been found to have an important role for the C−C bond forming transition state from the allyl-ethene complex (Scheme 9). The labile group's involvement allows Ni(II) to have a four-coordinated intermediate, and therefore the total activation energy is only 12.4 kcal/mol. The lowest path is shown in Scheme 9. Catalytic precursor **3** incorporates ethene to become **16**. The C−C coupling ensues via **17**, **18**, and **19** to rest at **20**. *The square-planar intermediate* **20** *is very low in energy, thanks to C−C bond formation, and represents one of the conformers for the lowest intermediate in the initiation path*. Note that **17**, **18**, and **19** (Scheme 9) are very close in the potential energy surface and represent virtually the same species, so the unique

Scheme 9. Generation of the Active Catalyst: (II) The Lowest Initiation Path

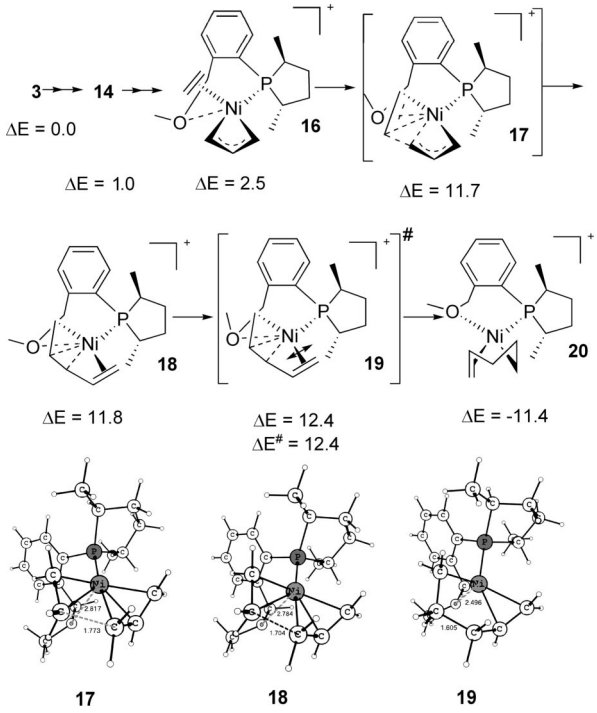

C−C agostic complex **18** does not deserve much attention.[17] For an alternative path having fewer steps from the precursor **3**, the activation barrier is just 0.3 kcal/mol higher (see **S10**, Scheme S3, $\Delta E^{\#} = 12.7$ vs $\Delta E^{\#} = 12.4$ for **19** in Scheme 9). None of the attempts to identify a viable transition state for a C−C bond formation from model complexes (with ligand PH_3) having no hemilabile group were successful, further emphasizing the disadvantage of a transition state leading to a three-coordinated intermediate. The involvement of the hemilabile group as the fifth coordination in **16**−**19** for lowering the C−C coupling barrier has experimental precedence.[18] We consider that the lack of reaction[3b] with ligand **4** under identical conditions depicted in Scheme 2 could be attributed to this effect, although decomposition of the catalyst is observed due to lack of coordination (only three-coordinate) during its preparation; thus its presence in the reaction medium is doubtful.

Next we understood why styrene, the other olefin present in the solution and relatively more abundant, cannot be involved in initiation. Styrene, in fact, is inherently more advantageous for the C−C bond formation because of its delocalization, as has been confirmed by model studies (Scheme S4). However, with the actual ligand, possibly due to steric effects between the phospholane Me with Ph of styrene, the corresponding transition state is higher in energy (**21**, Scheme 10) and the activation energy increases by 3.3 kcal/mol, making it kinetically noncompetitive. Note that no trace of C−C coupling products at the methylene carbon of styrene has been observed. The other styrene route, via **22**, is difficult, as expected mainly due to conjugative disadvantage. Unlike **22**, the coordinately unsaturated Ni can derive additional stabilization from being at the benzylic position in **21**.

(17) **18** is slightly lower than **17** in energy without ZPE correction.

(18) Pentacoordinate Ni-intermediates have been implicated in C−C coupling reactions and reductive eliminations, see: (a) Shultz, C. S.; DeSimone, J. M.; Brookhart, M. *J. Am. Chem. Soc.* **2001**, *123*, 9172. (b) Tatsumi, K.; Nakamura, A.; Komiya, S.; Yamamoto, A.; Yamamoto, T. *J. Am. Chem. Soc.* **1984**, *106*, 8181. Chemistry of five-coordinate Ni(II)-allyl complexes: ref 16a.

Scheme 10. Lowest C−C Coupling Transition States with Styrene for Initiation

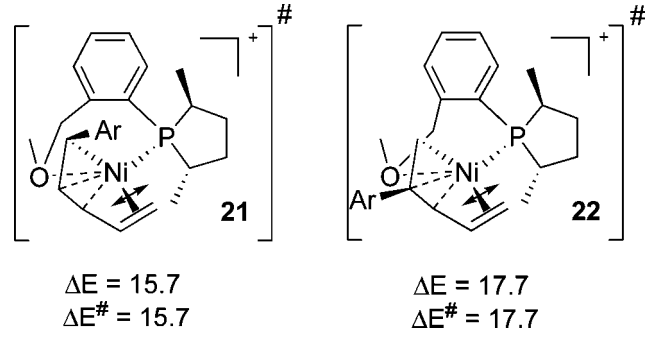

Catalyst Resting State in the Initiation Stages. The energetically most accessible intermediate, **20**, has three other isomers, as shown in Scheme 11. All four isomers (**20**, **23**, **S11**, and **24**) are close in energy, and **24** is the lowest; it could easily be obtained from **S11**, which is the direct outcome of the path involving **3** having fewer steps (vide supra, Scheme S3). Transition state **26** is a simple C−C flipping in the pentenyl chelate and hence has a small barrier, as is the case for transition state **25**, which gives **23** starting from **20**. The lowest intermediate, **24**, can also be arrived at from **20** through the transition state **29** with an activation energy of 17.7 kcal/mol. This requires many steps, as represented in Scheme 11. An agostic C−H···Ni (cf. **28**) needs to be invoked first, which is accomplished by the transition state **27**. Subsequently through transition state **29** another intermediate with an agostic interaction, **30**, is formed. Now the steps repeat in a reverse sense via the transition state **31** to yield the square-planar pentenyl chelate **24**, with the olefin trans to phosphorus. Although 17.7 kcal/mol is the highest barrier of the reaction up to this point, it is lower than the pentadiene's exit transition state (see below); thus we conclude that **24** is the resting state of the catalyst during initiation.

A Surprise. The Expected *β*-Hydride Elimination Has an Unacceptably High Barrier. The usual β-H elimination, assumed to be the route for the exit of pentadiene (**D** → **E** in Scheme 3), has been found to have a high barrier of 33.8 kcal/mol (Scheme 12). This is most possibly due to the trans effect. Hydride does not favor being positioned trans to the sole strong ligand P, but this path demands such an arrangement. Note that the hydride **33** and the transition state to this species, **32**, are prohibitively high in energy. That is, the weak stabilization of the metal−hydride bond by no means compensates the breaking of the C−H bond and losing a strong cis P−Ni−alkyl arrangement.

To circumvent these disadvantages, an alternative path was explored where the hydride can be brought to a position cis to the phosphorus. This route begins by a pseudo-trigonal-pyramid transition state, **34**, to reach the square-planar complex **35**, where the alkyl group is positioned trans to the phosphorus.[19] A look at the relative energies of square-planar structures **24** (−12.2 kcal/mol) and **35** (−2.7 kcal/mol) shows the effect of the trans effect. The difference of 9.5 kcal/mol clearly reveals that in the square-planar geometry the metal−alkyl bond prefers to be cis and the olefin trans to the phosphorus vis-à-vis the opposite arrangement, in which the olefin is cis to the phosphorus. β-Hydride elimination has to proceed through the intermediate **35**. In the transition state (**36**) leading to β-hydride elimination there is an alkyl group trans to P (*destabilizing*) and the stabilizing cis olefin has been separated from the metal, thus effectively creating a vacant site at the cis position. So this transition state corresponds to a large barrier of 27.9 kcal/mol

Scheme 11. Generation of the Active Catalyst: (III) Reaction Path to the Lowest Intermediate during Initiation

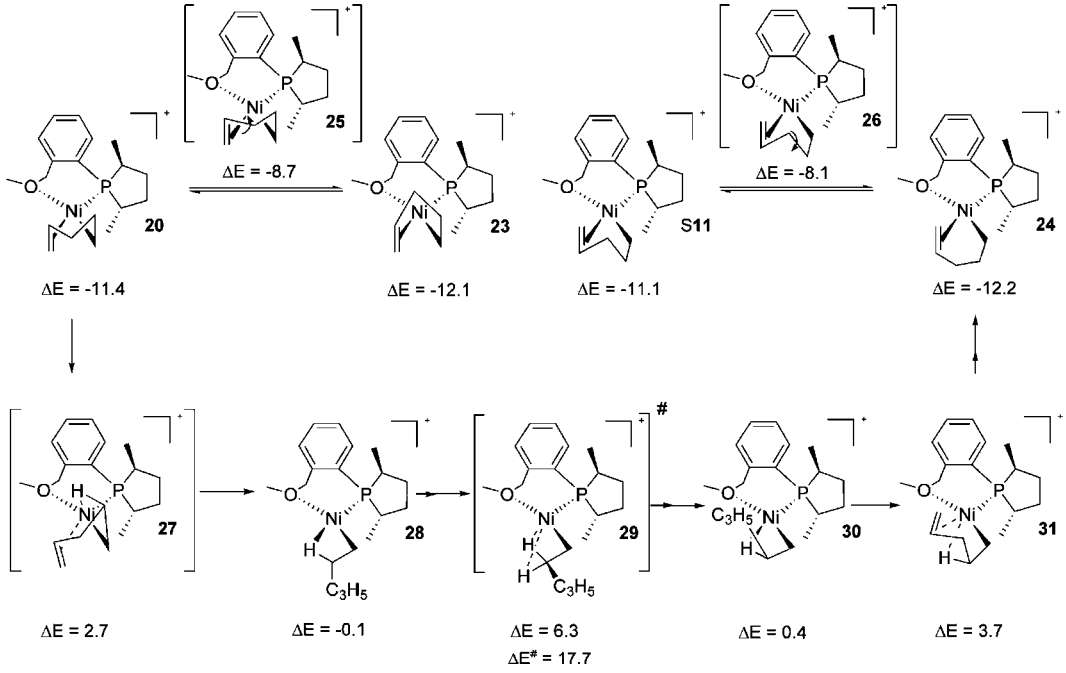

Scheme 12. Energetics of the β-Hydride Elimination Pathway

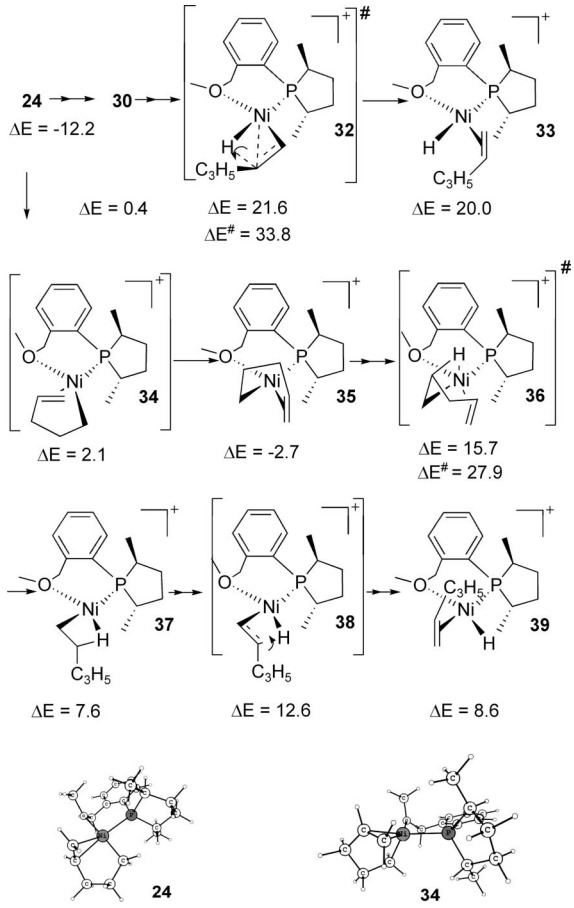

in creating a relatively stable agostic complex, **37**. As anticipated, the C−H bond breaking transition state **38** to form the cis hydride **39** is considerably lower than the corresponding transition state **32**, formation of which would appear to be more straightforward from the resting state **24**. The large difference between the energies of the two hydrides **39** and **33** is yet another manifestation of the trans effect. Thus this alternate path decreased the barrier of β-hydride elimination of pentadiene from 33.8 kcal/mol (**24 30** → **32** → **33**) to 27.9 kcal/mol (**24** → **35** → **36** → **39**). However, both processes are still large for a reasonable reaction rate at −45 °C. So we are forced to explore alternate paths for this key step in the generation of the active catalyst. This is described in the next section.[20]

A Possible β-H Transfer? Since all viable intermediates (**20**, **23**, **24**, or **S11**) have three coordination sites (except the site occupied by the phospholane ligand in the square-planar d^8 complex) usable for reaction, we explored how they can be utilized in avoiding energetically costly positioning of the hydride or alkyl group trans to P. Can alternate paths be found that decrease the barrier for 1,4-pentadiene's exit? We conceived that a transfer[21] of the β-H to another olefin positioned at the vicinal position to P (cis) bypasses the problem of having an alkyl/hydride intermediate formed trans to P. The lowest H-transfer transition state for the exit of 1,4-pentadiene is shown in Scheme 13.

In Scheme 13, the putative β-hydride resulting from the expulsion of pentadiene is transferred directly to the styrene. It must be remembered that even in the "free metal hydride" path (**D** → **E** → **F** → **G** in Scheme 3) the hydrogen needs to be added to styrene for the hydrovinylation to proceed; thus transition state **40** in fact decreases the number of required steps in comparison to the "free" hydride path. Note that in this scheme the incipient η^1-benzyl is being formed at a position

(19) It may be noted that the transition state **34** is very much lower in energy than isoelectronic analogues, for example, tetrahedral **10** (Scheme 6), where η^3-allyl was not flexible enough to make room for the ligand substituents as in **34**, which may be considered as a trigonal pyramid (rather than tetrahedral), with olefin in the plane of P and O (Scheme 12).

(20) For a similar result in the computational studies of Ni(II)-catalyzed polymerization/oligomerization of ethylene, see: (a) Deng, L.; Margl, P.; Ziegler, T. *J. Am. Chem. Soc.* **1997**, *119*, 1094. (b) Deng, L.; Woo, T. K.; Cavallo, L.; Margl, P. M.; Ziegler, T. *J. Am. Chem. Soc.* **1997**, *119*, 6177. (c) Musaev, D. G.; Froese, R. D. J.; Svensson, M.; Morokuma, K. *J. Am. Chem. Soc.* **1997**, *119*, 376. (d) Musaev, D. G.; Morokuma, K. *Top. Catal.* **1999**, *7*, 107. (e) See also ref 21.

(21) (a) Fan, L.; Krzywicki, A.; Somogyvari, A.; Ziegler, T. *Inorg. Chem.* **1996**, *35*, 4003. (b) Fan, L.; Krzywicki, A.; Somogyvari, A.; Ziegler, T. *Inorg. Chem.* **1994**, *33*, 5287.

Scheme 13. The Lowest Transition States for the Exit of Pentadiene

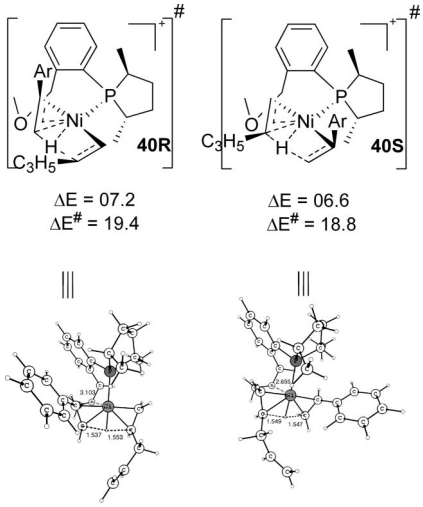

cis to the P, a favorable situation. Further, there is no genuine Ni−H bond. Both of these bonding situations enable decreasing of the barrier. Since a new chiral center is created, we have two diastereomeric possibilities. The energy of the transition state **40S** is 18.8 kcal/mol, and it is 19.4 kcal/mol for the transition state **40R**. Since no alternate lower route for the pentadiene's exit could be located, and the barrier 18.8 kcal/mol is the highest among all steps in the initiation, transition state **40** corresponds to the rate-determining (turnover-limiting) step during the initiation stage. Although a model study (Scheme S5) also suggests that styrene has an inherent advantage to accept the transferred H, because of the possibility of steric repulsion in the actual case, we examined how ethene fares. The corresponding ethene transition states in the real system are slightly lower, but for the hydrovinylation to carry on, another H-transfer to styrene needs to ensue. These energies, though small (activation barriers 19.1 and 19.8 kcal/mol for **S** and **R**, respectively; see Scheme S6), are still higher than for the formation of **40R** and **40S**. It is assumed that two such discontinuous high-energy transition states would not be preferred over a single transition state. Besides, the concentration of ethene is lesser than styrene in the successful reaction conditions (cf. Scheme 2). Similar is the situation for the H-transfer to styrene with the alternate regioselectivity, where the second H-transfer has a barrier of 20.5 and 20.9 kcal/mol, respectively, for **S** and **R** (Scheme S6). The lowering in energy of **40** with respect to the above-described second H-transfer has been ascribed to the C−H---π hydrogen bonding possibility with the pentenyl double bond and styrene's tail C−H.[22]

Since styrene is involved at this stage and the H-transfer decides the enantioselectivity, we will comment on it. As displayed in Scheme 13, **40S** is preferred slightly over **40R**, which means during initiation there is an advantage for the **S** isomer (benzyl-Ni complex), but since the amount of active catalyst precursor **3** is only about 1 mol %, this outcome has little bearing on the final enantioselectivity of the reaction. The slight disadvantage of **40R** is likely to be steric in origin, even though we cannot exactly pinpoint the particular groups in the complexes due to the fact that the ligand system is very flexible.

Scheme 14 depicts the details of the transformations that lead to **40** from the resting state **24**. Approach to the transition state **40R** from **24** is quite straightforward as shown. A direct substitution at **24** is not possible due to steric effects that prevent styrene π-electrons to make a close approach to the metal required for a concerted path. But **40R** can be reached readily as follows: styrene can be incorporated into **30** (see Scheme 11), an intermediate with an agostic Ni···H bond alluded to earlier via transition state **41**. Even though the agostic H in **30** removes some of the potential steric problems mentioned above, styrene replaces agostic H rather than O in a concerted fashion to give **42**, because the trans agostic H is weaker than cis O and because there are fewer steric problems (farther from the rest of the ligand) associated with its replacement. Now a turnstile rotation (**43**) involving agostic H, styrene, and the hemilabile O results in **44**, the penultimate intermediate for the transition state **40R**.

Reaching the corresponding **40S** requires many more steps since the phospholane ligand is not able to rotate easily along the P−Ni bond when the coordination sites are occupied. But **40S** can be attained as follows: unlike **41**, styrene replaces the agostic H of**30** in the required **S** fashion from the bottom (**45**) to reach the square-planar **46**. Note that these square-planar styrene complexes are not as favored as the chelate pentenyl **24** ($\Delta E = -12.2$ vs -7.4 and -10.0). Now a pseudo-trigonal-pyramid transition state, **47**, similar to the previously described transition state **34**, brings the system to **48**. In contrast to **34**, **47** fails to yield a square-planar structure directly because, instead of the restricted chelate in **34**, two separate species are involved here, and so there are other intermediates possible before the square-planar intermediate. Intermediate **48** may be considered, at least for book keeping purposes, as a square pyramid with the P, styrene, agostic H, and O defining the square plane. The penultimate intermediate of the H-transfer transition state, **50**, can be arrived at via **49**, which may be regarded as the axial alkyl of the square-pyramid **48** replacing the hemilabile O at the cis position. It is clear from the energies in Scheme 14 that a flexible hemilabile group is required not only for providing the third active site for the H-transfer but to arrive at the transition states **40**. A more rigid group would have rendered some of the transition states more energetic, and thus difficult to access.

The next lowest intermediate after the above crucial H-transfer transition state is η^3-benzylic **51** (Scheme 15). The intermediacy of η^3-benzylic species has been assumed from exclusive regioselectivity (Ni placed at the benzylic position), which will be described in the next section. The η^3-benzylic intermediate **51** can be reached as shown in Scheme 16. For **51R**, first the transition state **53** takes the immediate intermediate from **40R**, viz., agostic **52**, to η^3-benzylic **54** with pentadiene still attached in the cis position. The η^3-benzyl **54**, like η^3-allyl, further undergoes a turnstile-type rotation, **55**, effecting the pentadiene's exit and O's coordination to reach **51R**. An analogous pathway from **40S** leads to η^3-benzylic **51S**. The immediate intermediate of the H-transfer transition state, **56**, changes to η^3-benzylic **58** via transition state **57**, a transition state from η^1-benzyl agostic to true η^3-benzylic. Pentadiene exits from **58** by η^3-benzyl rotation (**59**).

Note that, although the η^3-benzylic is not as strong as η^3-allyl and is replaceable readily by an olefin, any olefin substitution has been found to be higher in energy due to steric effects from cis η^1-benzyl. So **51** is the lowest intermediate before any C−C coupling but is *not the resting state since the lowest intermediate in the catalytic cycle comes only after the C−C bond formation thanks to the energy lowering achievable by a new C−C bond (Figure 2, vide infra)*. It may be

(22) For a review on C−H---π hydrogen bonds in organic reactions, see: Nishio, M. *Tetrahedron* **2005**, *61*, 6923.

Scheme 14. Reaction Path to Reach 40 from 24

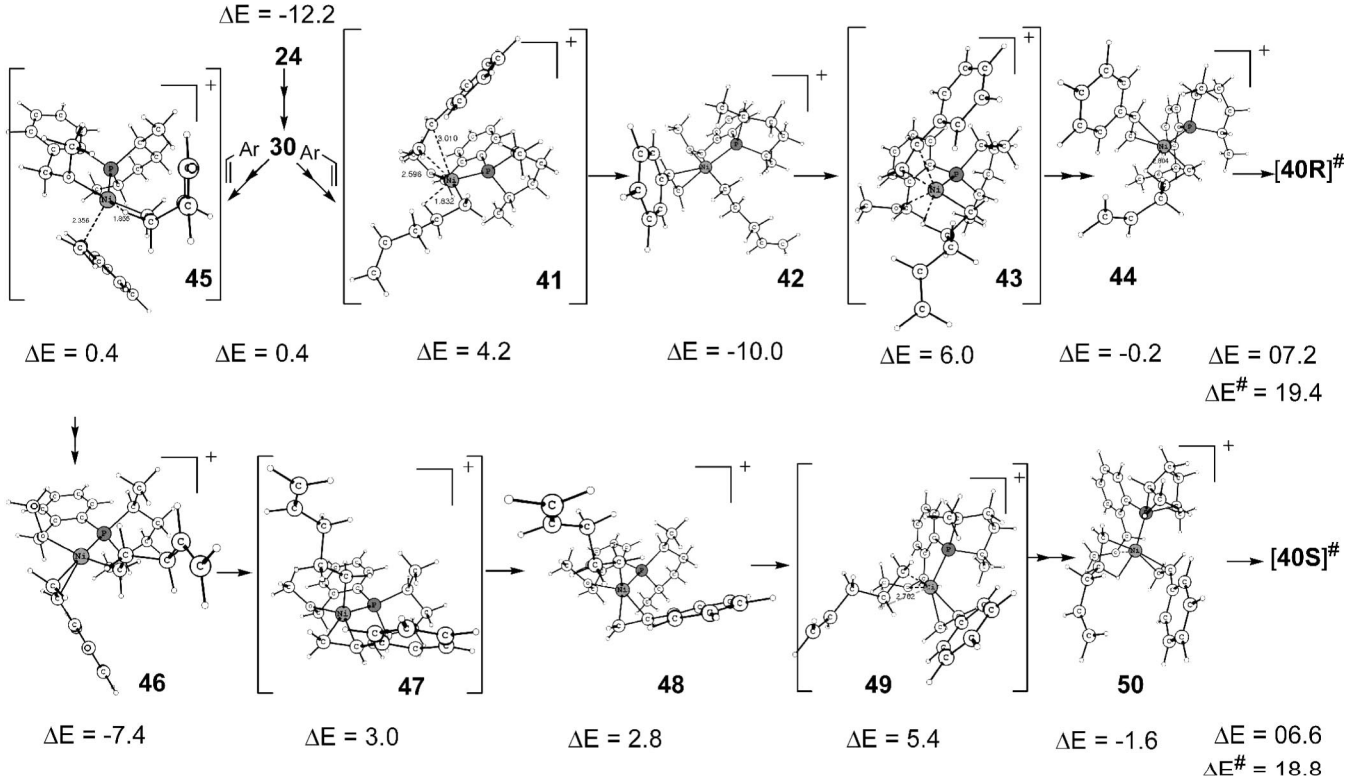

Scheme 15. η^3-Benzylic Intermediates

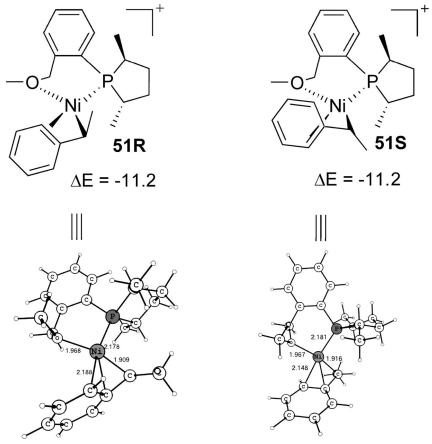

emphasized that there is no clear-cut demarcation possible from initiation to actual reaction, as the real reaction starting at the point of styrene incorporation though the initiation was formally completed only at the exit of 1,4-pentadiene.

Propagation of Catalytic Cycle

Carbon−Carbon Bond Formation via the η^3-Intermediate. The stage is set for the key carbon−carbon bond formation of the hydrovinylation reaction. Transition states **60R** and **60S** shown in Scheme 17 are the lowest for the C−C coupling. Thanks to the ability of phenyl to adopt multiple (η^4 and η^6) ligations, the barrier is only around 12 kcal/mol from the η^3-benzyl intermediates. This situation is somewhat similar to the C−C coupling process in the initiation, where the hemilabile "O" helped the coordination problem; here the phenyl group itself can accommodate the needed changes. In fact reaching **60** involves a slightly higher barrier (Scheme 18), which still is much lower than the previous H-transfer; thus once **40** is crossed, it is effectively a downhill move and thus the small difference in energy for **60R** and **60S** also has no role in affecting the enantioselectivity of the overall reaction.

A look at the structures **51** and **60** makes it clear that many steps are needed to attain the C−C bond forming transition state. The first required step is to change the η^3-benzylic orientation so that the sigma-bonded C, which undergoes reaction, is positioned trans to the phosphorus. Such a cis−trans conversion is difficult by the default tetrahedral transition states, which have barriers of 21.2 and 22.8 kcal/mol, respectively, for **R** and **S** (Scheme S7). We already know that a flexible olefin and alkyl together lowers the barrier for cis−trans interconversion (cf. **34** vs **10**).[19] In this case also, such a route involving ethene has been located. The trigonal-pyramid transition states **63** and **71**, respectively, for **R** and **S** will accomplish this (Scheme 18). The resemblance of **63** and **71** to **34** rather than to **13** is another exemplification of the differences of η^3-benzyl and η^3-allyl ligands, the former being part of an aromatic system, where the π coordination is weak.

The η^3-benzylic **51R** can incorporate ethene as in **61** to give **62**, which may be considered as a square pyramid with ethene in axial position. It may be noted again that unlike η^3-allyl, η^3-benzyl easily undergoes a synchronous transition for the reason described above. Intermediate **62** then goes through the trigonal-pyramid transition state **63** to reach **64**, which is an almost perfect square-planar complex. Now ethene has to move into the left cis position from the right position now occupied to reach the lowest C−C coupling transition state conformation (**60R**). This is possible to accomplish by ethene first getting ejected out and then substituting hemilabile O in the next step. Since the ethene needs to be replaced from the cis position, the barrier is high, and higher than **63**, so we searched for a route where ethene does not separate from the complex. In this path the square-planar **64** changes to square-pyramid **66**, which is similar to **62** but with ethene in the opposite axial position. Now

Scheme 16. Reaction Path to η^3-Benzylic Intermediates

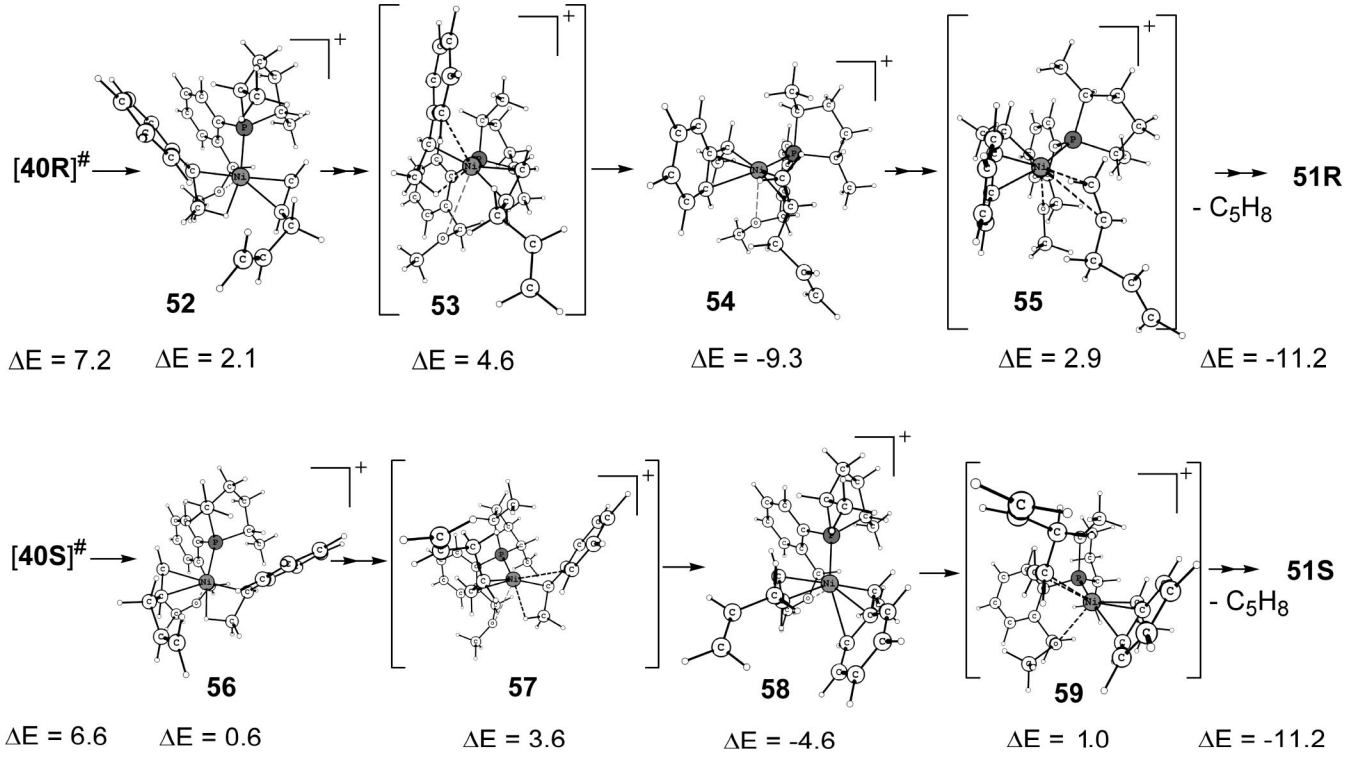

Scheme 17. Transition States for C−C Bond Formation

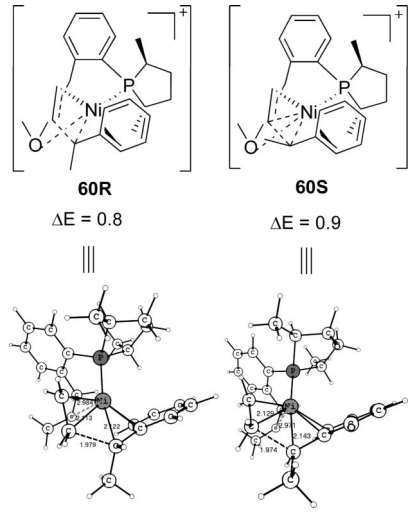

this axial ethene replaces the cis O via **67** to attain **68**, the penultimate intermediate of **60R**.

The intermediate **51S** analogously incorporates ethene to become a square-pyramid intermediate and is changed to square-planar **70** for the trigonal-pyramid transition state **71**, the highest transition state in this path. The immediate square-planar intermediate **72** passes through a rotational transition state **73** to arrive at the square-pyramid intermediate **74** (analogous to **66**), which then removes the hemilabile O to yield **76**, the intermediate before for C−C coupling.

Note that, as mentioned earlier, the transition states **63** and **71** are slightly higher than the C−C coupling, but both are lower than the previous H-transfer transition states; therefore we did not attempt any additional search for further lowering of this route, which anyhow appears to be unlikely. So in Figure 2 the C−C bond forming transition state is shown, and the peak labeled **60** represents the minimum barrier for the coupling.

Regioselectivity. The absence of the formation of linear product and oligomerization/polymerization may now be understood. Scheme 19 shows transition states for the C−C coupling process (**77**−**82**) for ethyl with ethene and styrene—the substrates of the title reaction—in comparison with **60R**. We chose ethyl as a representative of any possible alkyls that may be generated under the reaction conditions. Whether with styrene or ethene, or whether from cis or trans, the transition states **77**−**82** are all at least 4.9 kcal/mol higher than C−C bond forming transition state **60R** for the hydrovinylation reaction. So, kinetically, they are simply not competitive. The reasons for the disadvantages of all other C−C bond forming transition states other than that involved in a η^3-benzylic species can easily be attributed to the trans effect and loss of coordination. Note that **80**, **81**, and **82** are way too high in energy, as the incipient sigma metal−carbon bond is trans to phosphorus. For **77**, **78**, and **79** the only agostic H at trans position in the intermediate after the transition state is no match for an η^6 (or other polydentate) bonding possible with **60**.

For the mechanism to be rigorous, one has to consider whether **77**−**79** could be species present under the reaction conditions. Then the barriers for **78** and **79** are only 1.6 and 2.2 kcal/mol higher than the H-transfer transition state for the exit of pentadiene, **40S**, and **77** is 0.9 kcal/mol lower than **40S**. As a matter of fact, ethyl can form via an H-transfer from the pentadiene, which is 1.1 kcal/mol lower than **40S** (vide supra). So a question may arise as to why **77**−**79** were not observed, since ideally a difference of about 3 kcal/mol excludes only a competitive path. We consider some of the reasons that the results in Scheme 19 will suffice to conclude that no other C−C coupling paths are competitive and to account for the fact that experimentally no other C−C coupling reaction is observed. (a) Computational limitation: comparisons of different kinds of transition states are less accurate than the same kinds of transition states, so the systematic error may be lowering the energies of transition states shown in Scheme 19 with respect to H-transfer transition states. (b) The assumptions involved in

Scheme 18. Reaction Path Leading to C−C Bond Formation

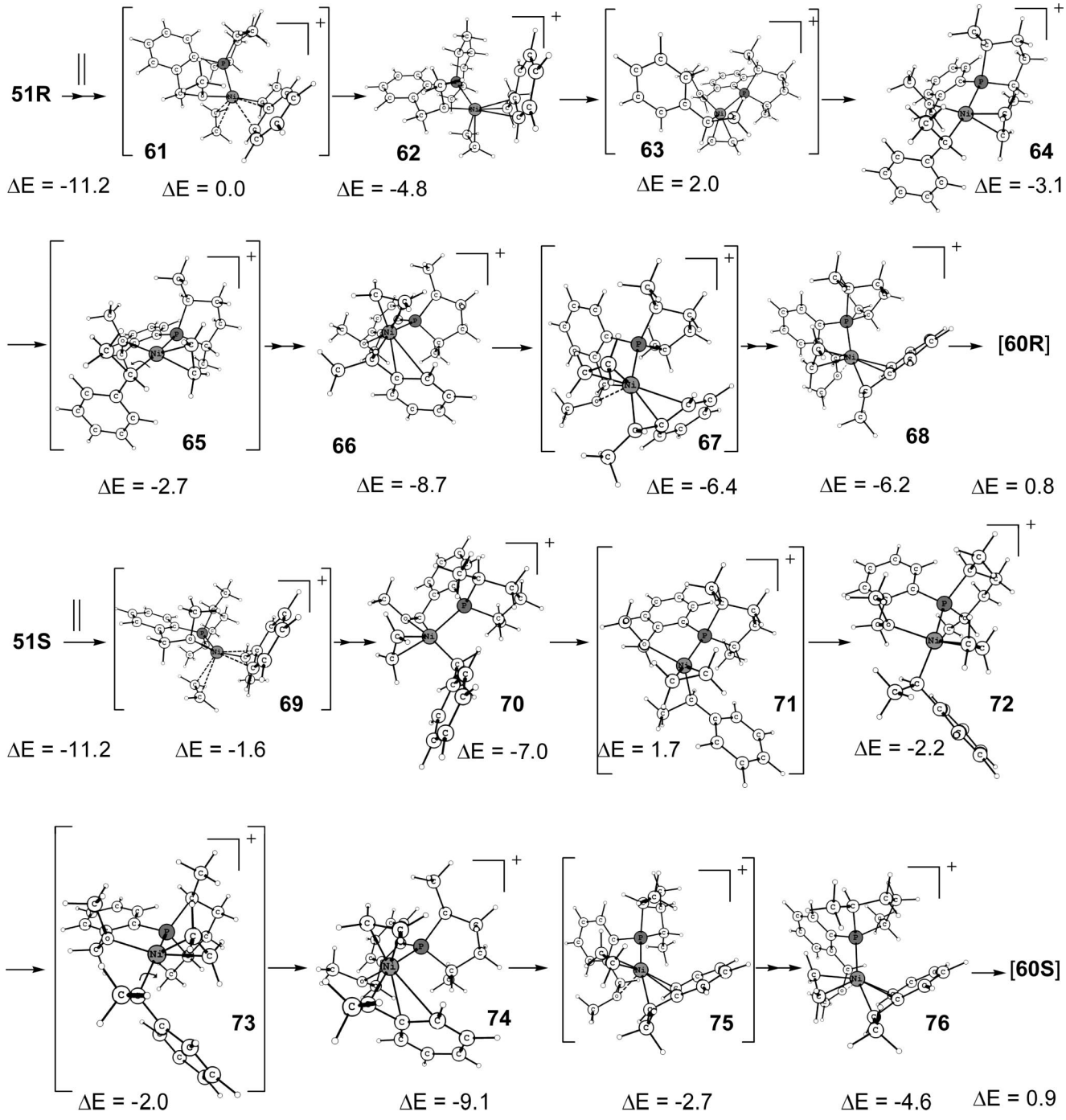

the transition state theory: the concept of a rate-determining step (in the case of a catalytic cycle, turnover-limiting step) is less valid when there are transition states of comparable energy. For **77**−**79** we already have the H-transfer transition state of comparable energy that is to be passed before the C−C coupling. Also there could be other comparable or higher transition states to achieve the path that leads to these C−C couplings. (c) The concentration of ethene is less in the solution; so practically, **77**, which involves two ethenes, is more difficult than the above data suggest. Note that with pentenyl, **83**, a transition state to be considered before the pentadiene's exit, the barrier for C−C coupling increased by another 2.8 kcal/mol. Transition states **78** and **79** indicate that styrene is less likely to undergo C−C coupling due to steric effects, so with pentenyl they all make it more than 3 kcal/mol higher than **40S**. Similar to **83**, the linear hydrovinylation transition state **84** is 4.9 kcal/mol higher than **40S** and hence not at all competitive. Transition states **85R** and **85S** are relevant after the hydrovinylation C−C coupling. They too are higher than the exit of hydrovinylation product (see below) transition states: **85R** by 3.2 kcal/mol relative to **99RS**, and **85S** by 2.0 kcal/mol relative to **99SR**. We conclude here that the trans effect and vacant coordination problem control the regioselectivity; so the exclusive outcome in the reaction, thanks to our custom-made catalyst, is hydrovinylation. It must be remembered that Ni(II) is versatile in C−C coupling ability and different ligand systems lead to different regioselectivity. So unlike oligomerization[23] and polymerization,[24] hydrovinylation requires a hemilabile group and a strong trans-directing ligand so that we have the correct requirements of an easy exit of product by a β-H transfer (using three coordination sites)

Scheme 19. Trans and Vacant Coordination Effect for C−C Bond Formation

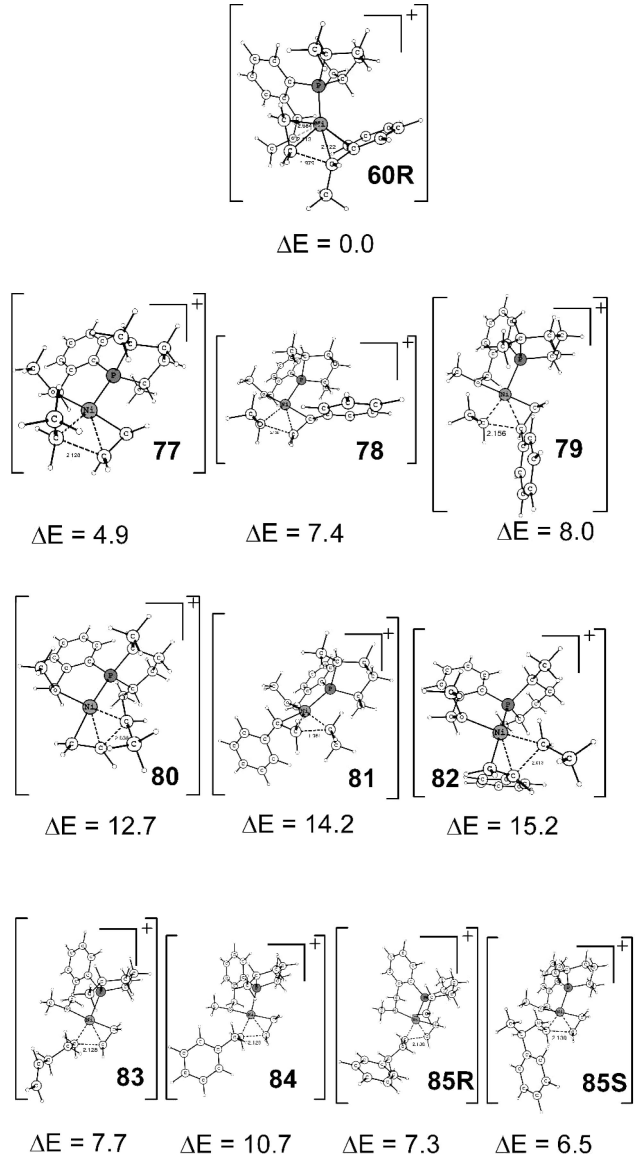

than any C−C coupling, except the one involving an η^3-allyl or η^3-benzyl (again using three coordination sites).

Exit of Product from Catalyst. Structures **86R** and **86S** in Scheme 20 represent the lowest intermediates after the C−C coupling, and the activation barrier for the exit of product should be measured from there. These intermediates can be reached as shown in Scheme 21. The immediate intermediates after the C−C bond formation are **87** (for **R**) and **93** (for **S**), which as described earlier may be considered as η^6 or η^4, effectively occupying the available two coordination sites in a square-planar complex.

Intermediate **87** from **60R** (and correspondingly **93** from **60S**) is readily convertible to η^2 structures, still maintaining tetracoordination via transition state **88** (and **94**). Unlike a strong olefin ligation in analogous **24**, η^2-coordination of phenyl is weak, and consequently the lowering of **89** (and **95**) is less than the changes in **24**, the resting state during initiation. Styrene or

Scheme 20. Lowest Intermediate before the Exit of Product

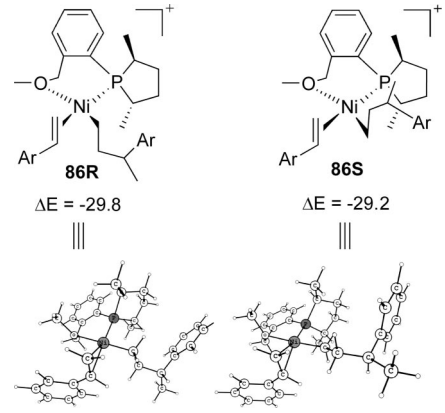

Scheme 21. Path Leading to the Lowest Intermediates

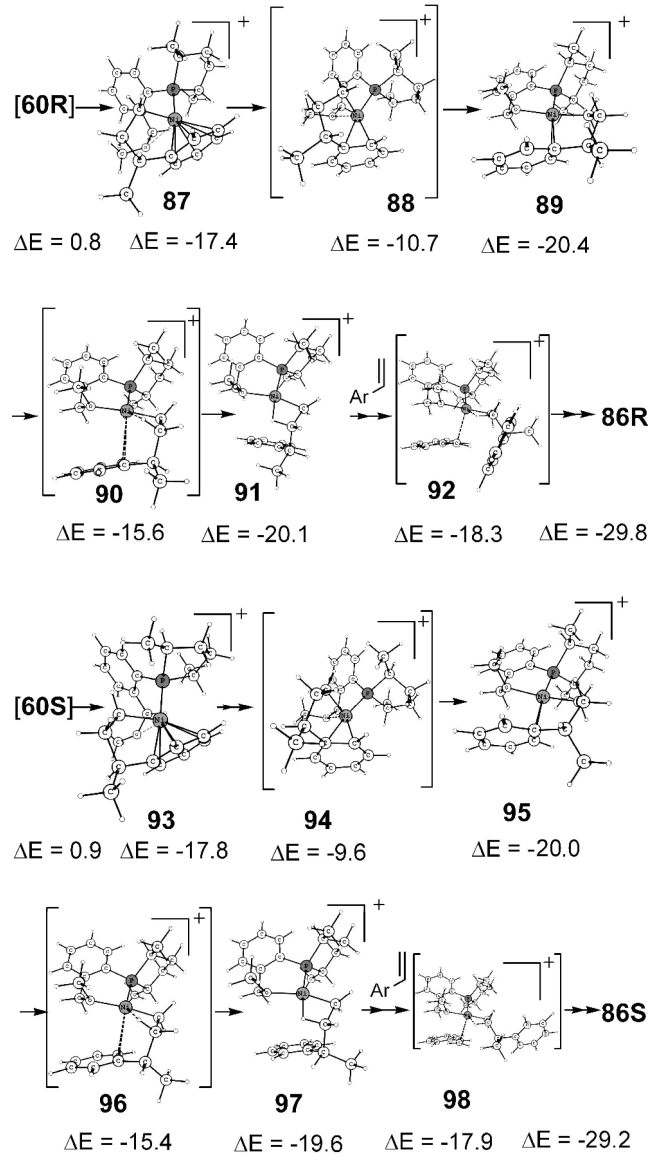

ethylene coordination more resembles **24**. We found styrene has a slight edge over ethene, and so **86** is the lowest intermediate. Intermediate **89** can easily support agostic stabilizations via transition state **90**. The same is true with **95** and **96**. Styrene incorporations in agostic **91** and **97**, respectively, for **R** and **S** isomers, lead to the lowest intermediates before the product's exit. Intermediate **86** is in fact the lowest state in

(23) Speiser, F.; Braunstein, P.; Saussine, W. *Acc. Chem. Res.* **2005**, *38*, 784.
(24) Ittel, S. D.; Johnson, L. K.; Brookhart, M. *Chem. Rev.* **2000**, *100*, 1169.

Scheme 22. β-H Transfer from Product to Styrene

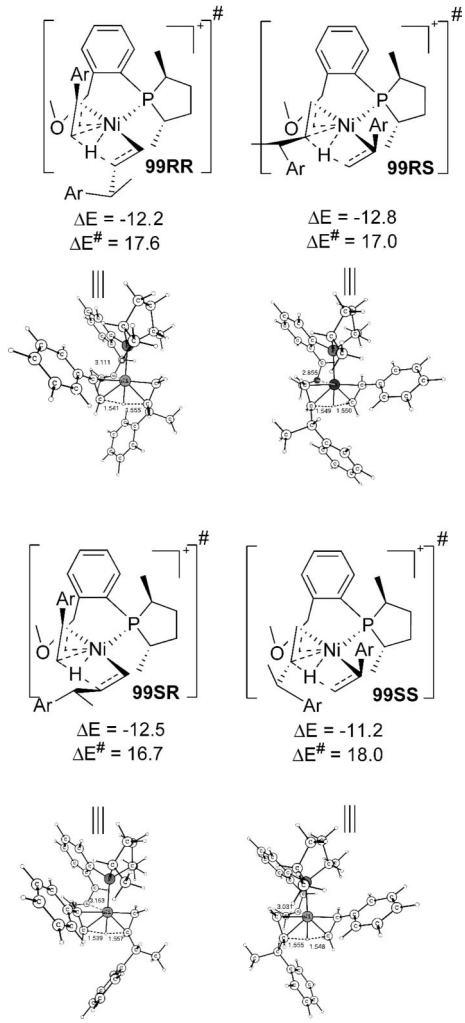

the catalytic cycle, and thus we assign this to be the *global* resting state of the catalyst.

Enantioselectivity. As expected from the forgoing discussion, the exit of product through a β-hydride route is prohibited. The barriers now are 32.6 and 31.3 kcal/mol for the direct path for **R** and **S** (Scheme S8). For the alternate β-hydride path the corresponding barriers are 23.0 and 22.8 kcal/mol (Scheme S8). The lowering of energy in this path compared to **36** in the initiation step is due to the ease of ethene to interact with cationic Ni(II) than the chelate olefin, which is not as flexible and so not positioned well. (Because η^2-phenyl is a very weak ligand, ethene intermediacy is required to lower the energy to the present value in this cis-hydride path.)

The rate-determining *β-H transfer* transition states for the exit of product are shown in Scheme 22. The barrier here is lesser than that during the initiation, partially due to the fact that the intermediate **86** is not as low with respect to **99** as the chelate **24** is with respect to **40** (cf. Scheme 13) and may be partially due to the improved C−H---π interaction with phenyl over pentenyl. It is to be noted that the energy of **99SS** is the highest despite that styrene is positioned in the right cis coordination site, which is less congested. The reason is that, to maintain the hydrogen bond, the group has to orient as pictured and causes extra steric congestion with −O-Me at the bottom. Again, as in initiation, ethene intermediacy necessitates a second H-transfer transition state, which is higher in energy and more so than initiation thanks to a better hydrogen bond with Ph in **99** than is possible with pentenyl. Contrast the

Scheme 23. Modified Mechanism of Hydrovinylation of Vinylarenes

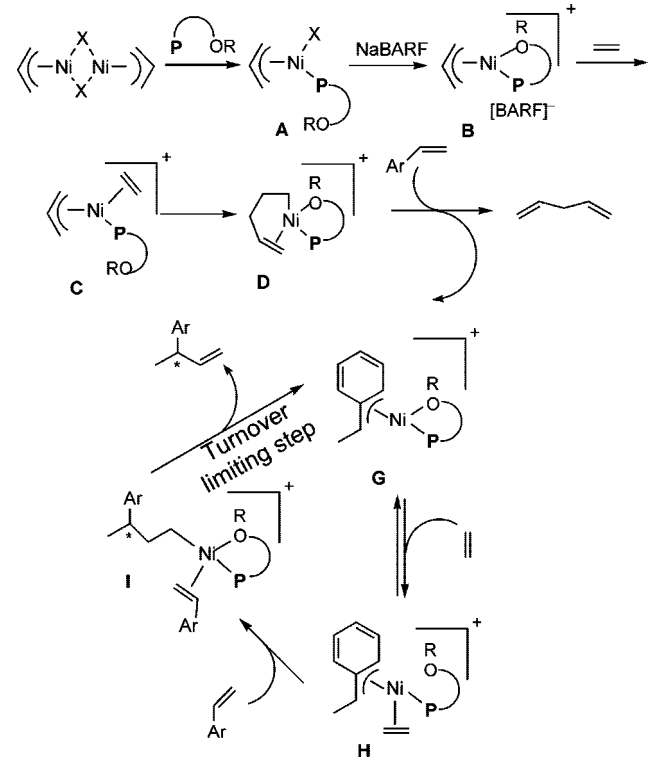

respective barriers displayed in Scheme 22 with ethene intermediacy barriers: **99RR** 19.6, **99RS** 18.9, **99SR** 19.0, and **99SS** 18.3 kcal/mol (cf. Scheme S6).

Since an intermediate with **R** configuration in the early stages of catalyst generation prefers to give the **S** product in the next C−C coupling stage, and vice versa (see Scheme 22), an estimation of the enantioselectivity is not straightforward. A detailed analytical derivation for the enantioselectivity based on the computational results on the barrier is beyond the scope of the present study. But it can be surmised that formation of **R** is easier than **S** because the resting state **86S** is higher than **86R** and because **96SS** is unfavorable. Or to put in a less rigorous way, the average activation barrier leading to product **R** (17.2 kcal/mol) is lower than that of **S** (17.5 kcal/mol). So we conclude that the computation, despite its limitations, faithfully reproduces the experimental trend for enantioselectivity thanks to the protocols used in the calculation, which compares similar transition states along the reaction coordinates, thereby eliminating many of the errors. Since the enantioselectivity is determined by steric effects in a composite way due to the flexibility of the ligand system, even a simple modification in the ligand could alter the energies of various transition states in this complex reaction, and this has been experimentally validated.[2,3] It is premature to suggest suitable candidates for better enantioselectivity without doing adequate calculations on the new reaction path for each of the proposed ligands.

The path leading to transition states **99** and the formation of η^3-benzylic **51** from the transition states are similar to the corresponding path involving the pentenyl intermediates described in Schemes 14 and 16, respectively. These paths are given in the Supporting Information as Schemes S9 to S12.

Summary and Conclusion

Figure 2 summarizes the reaction profile. Square-planar η^3-allyl complex **3**, the sole diastereomer of the active catalyst

present before the addition of olefins, reacts with ethene via transition state **19** to yield the square-planar **24**, which is the resting state during initiation. Pentadiene's exit from **24** involves the rate-determining H-transfer transition state **40**, which leads to η^3-benzylic **51**. The originally proposed β-hydride elimination requires prohibitively high energy, and we suggest that this is not feasible along the reaction coordinate. The activation barrier for the new initiation is 18.8 kcal/mol. The hydrovinylation reaction continues by the incorporation of ethylene at η^3-benzylic **51** and a subsequent low-barrier C−C coupling (**60**). Unlike **60**, any other C−C coupling has a much higher barrier due to the trans effect of the ligand and a resultant vacant coordination that explains the regioselectivity. The next lowest intermediate (the resting state), **86**, is attained by the incorporation of styrene. Exit of the product requires H-transfer transition state **99**, and this is the rate- and enantio-determining step for the reaction. The barrier of 16.7 kcal/mol is lower than that of initiation, and considering the effect of entropy excluded in the initiation barrier, computation suggests a definite induction period for the catalysis. The possible isomerization of product, a recurrent problem in metal hydride reaction paths and often observed with hydrovinylation reactions catalyzed by other metals such as Pd(II), is prevented because soon after the H-transfer transition state **99** it is a downhill process (cf. **99** → **51** → **60** → **86**). In other words, once the β-H of the product is transferred to styrene, there is no recovery for that hydrogen to transfer back to the product. Another interesting aspect of this reaction is that the configuration of the product present in one cycle affects the enantioselectivity in the next cycle, and so the enantiomeric excess of the product varies as the reaction progress.

An examination of the originally proposed mechanism (Scheme 3) reveals that most of the major conjectures remain in tact, the main difference being how the β-hydrogen from the η^1-Ni complex-carrying product (**I**, Scheme 3) is transferred to a new product. There is little support for the formation of a free-standing $[L_nNi-H]^+$ (**E**, Scheme 3). A concerted mechanism in which the H-transfer from **I** takes place directly to the prochiral faces of the styrene appears to be the path of least activation energy. However, this introduces a new complication in the mechanism in that the penultimate intermediate before ejection of the product has three chiral entities involved (e.g., **86**), two from the substrate and one from the ligand. The initiation involves the formation of two diastereomeric complexes (**51R** and **51S**) even before the prochiral faces of the substrate of the formal catalytic cycle are encountered, and these complexes are necessarily parts of a productive catalytic cycle, not a simple metal hydride (**E**, Scheme 3) as was initially assumed in the working model.

To accommodate these findings, we modify the original proposal as shown in Scheme 23.

In conclusion, we hope that the present study fulfills several gaps in our understanding of the hydrovinylation reaction. We expect this study to help with further mechanistic studies directed at improving the substrate scope, efficiency, and selectivity of this important reaction. Such studies are in progress.

Acknowledgment. We are grateful for the computational facilities at CMSD University of Hyderabad, MHPC Hawaii, and SERC Indian Institute of Science Bangalore. J.J. thanks CSIR for a fellowship. Financial assistance for part of the work done at The Ohio State University by NSF (CHE-0610349) and NIH (General Medical Sciences, R01 GM075107) is gratefully acknowledged.

Supporting Information Available: Schemes S1−S12 mentioned in the text, complete author list of ref 11, and Cartesian coordinates of all geometries reported. This material is available free of charge via the Internet http://pubs.acs.org.

OM900045P